

## Measurement of the Rate of Increase of Neutrino Cross Sections with Energy

R. Blair,<sup>(a)</sup> B. Barish, Y. K. Chu, B. Jin,<sup>(b)</sup> D. MacFarlane, R. L. Messner,<sup>(c)</sup> J. Lee,<sup>(d)</sup> J. Ludwig,<sup>(e)</sup>  
D. B. Novikoff,<sup>(f)</sup> and M. V. Purohit

*California Institute of Technology, Pasadena, California 91125*

and

P. S. Auchincloss, F. Sciulli, and M. H. Shaevitz

*Columbia University, New York, New York 10027*

and

F. Bartlett, D. Edwards, H. Edwards, H. E. Fisk, Y. Fukushima,<sup>(g)</sup> Q. A. Kerns, T. Kondo,<sup>(g)</sup>  
P. A. Rapidis, S. L. Segler, R. J. Stefanski, D. Theriot, and D. Yovanovitch

*Fermi National Accelerator Laboratory, Batavia, Illinois 60510*

and

A. Bodek, R. Coleman,<sup>(h)</sup> and W. Marsh<sup>(h)</sup>

*University of Rochester, Rochester, New York 14627*

and

O. Fackler and K. A. Jenkins

*Rockefeller University, New York, New York 10021*

(Received 6 April 1983)

The energy dependence of the cross section for neutrino- and antineutrino-nucleon charged-current interactions has been determined from data taken in Fermilab's dichromatic neutrino beam.  $\sigma^{\nu}/E = (0.669 \pm 0.003 \pm 0.024) \times 10^{-38} \text{ cm}^2/\text{GeV}$  and  $\sigma^{\bar{\nu}}/E = (0.340 \pm 0.003 \pm 0.02) \times 10^{-38} \text{ cm}^2/\text{GeV}$  are found. These results are higher than some previous measurements.

PACS numbers: 13.15.Em

Measurements of neutrino-nucleon scattering at high energies have been very important in verifying the constituent quark model of the nucleon. In this model, which incorporates approximate scaling,<sup>1</sup> the charged-current cross sections for neutrinos and antineutrinos are predicted to rise almost linearly with beam energy; the slope of this rise ( $\sigma/E$ ) is related directly to integrals of the structure functions at fixed neutrino energy. We report here measurements of high-energy neutrino-nucleon cross sections which are higher than some previous measurements.<sup>2-6</sup>

Normalized neutrino cross sections are most accurately measured by using a dichromatic beam (i.e., from a momentum-analyzed  $\pi, K$  beam) as the neutrino source. The precision tends to be limited by uncertainties in flux measuring and calibration and by the event statistics. The high-statistics measurement presented here is based on a total event sample of 150 000  $\nu_{\mu}$  events. The experiment was performed in the Fermilab neutrino area (E616) using the NO dichromatic beam<sup>7</sup> and the Lab-E iron detector.<sup>8-10</sup> The flux was monitored by ion chambers that were calibrated

with several independent methods.<sup>11</sup>

The cross section in a specific energy range is given by the expression  $\sigma = N_{\text{ev}}/F_{\nu}N_n$ , where  $N_{\text{ev}}$  is the number of charged-current events occurring in some fiducial volume of the detector,  $F_{\nu}$  is the flux of incident muon neutrinos from the decay in flight of  $\pi$  and  $K$  mesons, and  $N_n$  is the number of target nucleons in this volume.

The flux ( $F_{\nu}$ ) is calculated from measurement of the number of pions and kaons and from their momentum and angular distributions. The beam of  $\pi$ 's,  $K$ 's, and protons was sign and momentum selected ( $\Delta p/p = \pm 9.4\%$ ) before it traversed a 350-m-long decay region. The relative populations of the particle types were measured with a focusing Cherenkov counter. Typical rms errors were 1% to 4% for pions and 4% to 7% for kaons.<sup>12</sup> The magnitude of the hadron flux was monitored by ion chambers at two separated locations along the decay region. The calibration<sup>12</sup> of these ion chambers is discussed in detail elsewhere.

The magnetic elements of the secondary beam line were energized under ten separate operating conditions to transmit and focus 120-, 140-, 168-,

200-, and 250-GeV/c positive or negative secondary hadrons. In the dichromatic beam, neutrinos from  $K \rightarrow \mu \nu_\mu$  populate energies near the hadron beam energy and neutrinos from  $\pi \rightarrow \mu \nu_\mu$  cover a range below 0.43 of the beam setting. Neutrino and antineutrino interaction events were collected over the energy range 30 to 250 GeV. The choice of settings permitted data with some overlap in neutrino energy from setting to setting. The cross sections from data in the overlapping energy ranges agree well.

The events ( $N_{ev}$ ) were detected with use of the Lab-E detector,<sup>8, 10</sup> consisting of a 640-ton target region 3 m  $\times$  3 m in cross section, with full-area calorimetry counters located every 10 cm of steel and spark chambers located every 20 cm of steel along the beam direction. Stringent fiducial cuts (e.g., the radius of interaction  $< 1.3$  m from the center of the square target) and upstream veto requirements assure that all interactions occurred well within the iron target material. Cosmic-ray events that survive these cuts comprise less than 0.5% of the sample as measured by recording data in the 10-sec intervals between the millisecond-long beam bursts. The remaining subtracted background, due to neutrinos born upstream of the decay region, was measured in runs with the entrance to the decay region blocked.

Charged-current interactions in the target contain a final-state penetrating muon and hadrons that produce a shower in the iron calorimeter. This calorimeter was used to measure the hadron energy and a downstream toroidal magnet was used to measure the muon momentum. The calibrations and resolutions of these devices were obtained in a test beam of hadrons and muons of known energy. (The standard deviations were  $\Delta E_h = 0.89\sqrt{E_h}$  and  $\Delta p_\mu = 0.11p_\mu$  with energy in gigaelectronvolts.) Figure 1 shows the energy distribution for a typical data sample at the 250-GeV/c setting in a limited fiducial volume of the target. The dichromatic nature of the beam is evident and the identification of  $\pi$ - and  $K$ -decay neutrinos is unambiguous.<sup>13</sup>

There were two separate triggers that responded to (a) the presence of a penetrating muon into the magnet downstream of the target ( $E_\mu > 10$  GeV and polar lab angle  $\theta_\mu < 100$  mrad); and (b) the presence of a minimum hadron energy deposition in the target ( $E_h > 10$  GeV) and a penetrating muon ( $E_\mu > 2.9$  GeV,  $\theta_\mu < 370$  mrad). These triggers were formed from completely independent counters and logic circuitry. Typical events ( $\sim 75\%$ ) were in a kinematic regime of trigger overlap al-

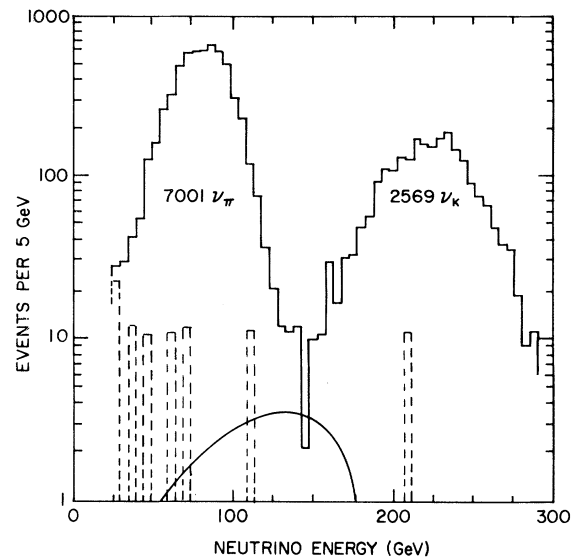


FIG. 1. Solid histogram: Distribution in observed total energy for events inside a single radial bin of interaction points at the target ( $25.4 \text{ cm} < R < 50.8 \text{ cm}$ ) for the +250 GeV/c fast-spill data. This separation is typical of data at all radii and beam settings. (Note the logarithmic scale.) Dashed histogram: Observed energy distribution for events obtained when the entrance to the decay region is blocked (wide-band background). These data have been normalized to the same number of incident protons as the data in the solid curve. Smooth curve: Calculated  $\nu_\mu$  events from  $K_{\mu 3}$ -decay neutrinos, normalized to the events in the  $\nu_K$  peak.

lowing constant monitoring of trigger efficiencies. These were greater than 99% in all cases. Corrections, for losses from azimuthal inefficiencies for observing the muon, were calculated by a simple geometric rotation on an event-by-event basis. These corrections averaged less than 6% in magnitude. The measured events cover essentially all kinematic possibilities in this neutrino energy region, in an unbiased fashion,<sup>2</sup> for  $\theta_\mu < 370$  mrad. Corrections for large polar angles were made by calculations; they were generally small ( $< 6\%$ ), decreasing to  $< 1\%$  at higher energies. These corrections were insensitive to several different assumptions for the structure functions.<sup>14</sup> As an example, the cross section would change by less than 1% at all energies if we were to use fits to our data<sup>15</sup> as opposed to those published in Ref. 3.

The data presented here were taken during fast resonant extraction ( $\sim 1$  ms each machine cycle). The experiment could record only one event per machine cycle. The fraction of this beam to which the experiment was sensitive averaged 70%

during neutrino running and 90% during antineutrino running. This fraction was measured in two ways: by recording the flux during the triggerable and nontriggerable times, and by counting (but not recording) events during the nontriggerable time. The measurements of this fraction as obtained from the two methods typically agreed to 1%. Data were also taken during 1-sec-long extraction of the beam during neutrino running. The experiment was sensitive for 85% of the flux for these data. The neutrino cross sections obtained with these data agreed to 1% with that from the fast-resonant-extraction data.

Table I shows our estimates of the largest contributions to the systematic errors quoted for individual  $\nu_\mu$  and  $\bar{\nu}_\mu$  cross-section values. Item (4) refers to possible misidentification of events as induced by  $\pi^-$  or  $K^-$ -decay neutrinos due to improper event reconstruction. Item (5) refers to flux uncertainties due to the spread in neutrino angles, limited by our knowledge of the rms angular spread of the parent hadron beam, as measured by position-sensing devices. The mean neutrino energy at a given target radius is determined in two ways: from the energy distribution of neutrino events and from the measurement of the mean momentum of the parent hadron beam. Item (6) was estimated from the agreement of the two techniques. In addition to the above errors, we have estimated an overall  $\pm 3\%$  scale error on the  $\nu_\mu$  cross sections and  $\pm 6\%$  on the  $\bar{\nu}_\mu$  cross sections (not shown in Fig. 2). This error includes the ion chamber calibration error and the uncertainty in applying this calibration to the

TABLE I. Approximate point-to-point errors in cross sections and their sources. Actual errors depend on energy setting and the position in the target.

Item	$\nu_\pi(\bar{\nu}_\pi)$	$\nu_K(\bar{\nu}_K)$
1. Statistical counting errors, including empirically subtracted backgrounds	3%	8%
2. Particle fractions ( $\pi/K/p$ )	(1-4)%	(4-7)%
3. Monitoring stability and calibration	(2-5)%	(2-5)%
4. Crossover of events, $\nu_\pi \leftrightarrow \nu_K$	0.7%	2.5%
5. Beam angular divergence errors	3%	2%
6. Neutrino energy error	1.5%	1.5%
7. Deadtime uncertainty	1%	1%

chamber and electronics used while taking data.

Figure 2 shows the neutrino and antineutrino cross sections divided by energy for the combined data. The inner error bars are statistical; the outer include the systematic errors of Table I. These cross sections contain small corrections ( $-2.1\%$  for neutrinos,  $+1.4\%$  for antineutrinos) to convert the iron-target values to those of a pure isoscalar target. The data shown in Fig. 2 for both neutrinos and antineutrinos are consistent with being independent of energy.<sup>16</sup> ( $\chi^2/\text{degree of freedom} = 0.5$  for antineutrinos and 1.2 for neutrinos.)

The average slopes from this measurement are  $(\sigma/E)_\nu = (0.669 \pm 0.003 \pm 0.024) \times 10^{-38} \text{ cm}^2/\text{GeV}$ , and  $(\sigma/E)_{\bar{\nu}} = (0.340 \pm 0.003 \pm 0.020) \times 10^{-38} \text{ cm}^2/\text{GeV}$ . The first error is statistical and the second systematic; the systematic error quoted includes the scale error mentioned above. The neutrino value agrees well with the cross-section slope obtained with use of 200-GeV/c and 300-GeV/c beam settings during an engineering run preparatory to this experiment<sup>9</sup>:  $(0.70 \pm 0.04) \times 10^{-38} \text{ cm}^2/\text{GeV}$ . However, these values are higher than some previously published results.<sup>2-6</sup> Many of the participants in this measurement also participated in the earliest measurement,<sup>2</sup> which was lower. The reasons for this difference are not fully understood. Several aspects of the experimental technique have been considerably improved. The beam line, flux monitoring, calibrations, and neutrino detection apparatus are

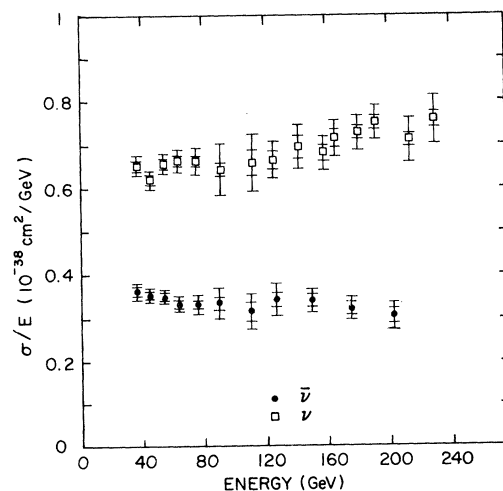


FIG. 2. Cross-section slope for neutrinos and antineutrinos vs energy for the data from this experiment. The values in this plot are available in Ref. 16.

completely new, and are more sophisticated. Substantial corrections to the flux-monitor values and for lost events applied to the earliest result were not necessary for the result reported here.

In summary, we find normalized high-energy neutrino and antineutrino cross sections to be higher than some earlier values. This result directly affects the fraction of momentum carried by struck quarks, as well as the normalization of quark-model sum rules and structure functions.

We would like to acknowledge the assistance of the Fermilab neutrino department and other departments at Fermilab during the preparation and execution of the experiment. This work was supported by the U. S. Department of Energy and the National Science Foundation.

---

<sup>(a)</sup>Present address: Columbia University, New York, N.Y. 10027.

<sup>(b)</sup>Present address: Institute for High Energy Physics, Peking, People's Republic of China.

<sup>(c)</sup>Present address: Stanford Linear Accelerator Center, Stanford, Cal. 94305.

<sup>(d)</sup>Present address: Sandia Laboratory, Albuquerque, N.M. 87185.

<sup>(e)</sup>Present address: Albert Ludwigs University, Freiburg, Federal Republic of Germany.

<sup>(f)</sup>Present address: Hughes Aircraft Co., El Segundo, Cal. 90245.

<sup>(g)</sup>Present address: National Laboratory for High Energy Physics, Tsukuba-gun, Ibaraki-ken 305, Japan.

<sup>(h)</sup>Present address: Fermi National Accelerator Laboratory, Batavia, Ill. 60510.

<sup>1</sup>R. P. Feynman, Phys. Rev. Lett. 23, 1415 (1969);

J. D. Bjorken and E. A. Paschos, Phys. Rev. 185, 1975 (1969).

<sup>2</sup>B. C. Barish *et al.*, Phys. Rev. Lett. 39, 1595 (1977).  $\sigma_\nu/E = 0.609 \pm 0.030$  and  $\sigma_{\bar{\nu}}/E = 0.290 \pm 0.015$ .

<sup>3</sup>J. G. H. deGroot *et al.*, Z. Phys. C 1, 143 (1979).  $\sigma_\nu/E = 0.62 \pm 0.05$  and  $\sigma_{\bar{\nu}}/E = 0.30 \pm 0.02$ .

<sup>4</sup>M. Jonker *et al.*, Phys. Lett. 99B, 265 (1981), and 100B, 520(E) (1981), and 103B, 469(E) (1981).  $\sigma_\nu/E = 0.604 \pm 0.032$  and  $\sigma_{\bar{\nu}}/E = 0.301 \pm 0.018$ .

<sup>5</sup>P. Bossetti *et al.*, Phys. Lett. 110B, 167 (1982).  $\sigma_\nu/E = 0.657 \pm 0.03$  and  $\sigma_{\bar{\nu}}/E = 0.309 \pm 0.016$ .

<sup>6</sup>T. Kitagaki *et al.*, Phys. Rev. Lett. 49, 98 (1982).  $\sigma_\nu/E = 0.68 \pm 0.11$ .

<sup>7</sup>D. A. Edwards and F. J. Sciulli, Fermilab Report No. TM-660, 1976 (unpublished).

<sup>8</sup>B. C. Barish *et al.*, IEEE Trans. Nucl. Sci. 25, 532 (1978).

<sup>9</sup>J. Lee, Ph.D. thesis, California Institute of Technology, 1980 (unpublished).

<sup>10</sup>R. Blair, Ph.D. thesis, California Institute of Technology, 1982 (unpublished).

<sup>11</sup>The flux measurement and background measurements (such as neutrinos from upstream sources) were provided to the two bubble-chamber groups (Hawaii-Berkeley-Fermilab and Brookhaven National Laboratory-Columbia-Rutgers) who accumulated data during part of the same running period.

<sup>12</sup>R. Blair *et al.*, Fermilab Report No. Pub-83/26-Exp, 1983 (to be published).

<sup>13</sup>For a detailed description of the method used to separate  $\pi^-$  and  $K^-$ -decay neutrino events, see Refs. 2, 9, and 10.

<sup>14</sup>H. E. Fisk and F. Sciulli, Annu. Rev. Nucl. Part. Sci. 32, 499 (1982).

<sup>15</sup>R. E. Blair *et al.*, University of Rochester Report No. UR-831, 1982 (to be published).

<sup>16</sup>A table of the values plotted in Fig. 2 is available in R. Blair *et al.*, Fermilab Report No. Pub-83/27-Exp, 1983 (unpublished).